THEORETICAL ANALYSIS OF HVAC DUCT HANGER SYSTEMS

R.D. Miller
NKF Engineering, Inc.

SUMMARY

The transmission of vibration from heating, ventilation, and air conditioning (HVAC) systems through a structure can be a potential source of unwanted noise in a ship or building. In order to effectively reduce the transfer of vibration from HVAC ducting to the supporting structure, the ducting may be supported with resilient hangers. This paper addresses methods which together can be used to analyze the harmonic response of an HVAC duct hanger system over an extensive frequency range. The finite element, component mode synthesis, and statistical energy analysis methods are demonstrated. Results for the duct hanger analysis are presented including vibratory response and power flow calculations. The methods are shown to yield reasonably close predictions for the frequency ranges for which predictions overlap. It was concluded that the overall methodology provides an efficient way to perform harmonic structural analysis over a wide frequency range.

INTRODUCTION

The overall methodology used to perform the analysis consisted of several mathematical techniques. Each method of analysis was employed for the frequency range it is best suited for. In this way, the analysis was performed very efficiently. The low frequency analysis (0-300 Hz) was performed with the finite element method (FEM) using NASTRAN. Standard finite element modeling of the system was performed in this frequency range. The mid-range (300-1,000 Hz) was analyzed using Component Mode Synthesis (CMS) with NASTRAN. For this analysis, the duct (a cylinder in this case) was modeled with generalized coordinates as a modal component. A pre-processor was developed to provide NASTRAN with the required generalized coordinate properties and modal expansions for the duct. The high frequency range (800-5,000 Hz) analysis was conducted with Statistical Energy Analysis (SEA) coupled with a closed-form harmonic beam analysis program. These techniques cover overlapping frequency ranges, therefore providing independent checks on each analysis. Following a brief discussion of each method of analysis, results for a typical duct hanger configuration are presented.

TECHNICAL APPROACH

The four methods used in predicting the harmonic response of a section of an HVAC ducting system with duct hangers are presented in the following paragraphs. The reason for using several techniques is to minimize cost and maximize accuracy and efficiency of the analysis. The CMS method plays a crucial role in that it economically bridges the gap between the FEM and SEA solutions.

Finite Element Analysis

The finite element method (FEM) is an excellent method for analyzing the harmonic response of a duct hanger system at low frequency. The code NASTRAN was selected for conducting the analysis (Reference 1). NASTRAN has a large amount of flexibility and is able to account for a high level of detail in structural modeling. With this method it is possible to model each component of the system with sufficient detail to accurately represent the modes in the low frequency range of analysis. Typically, at least 6 to 10 grids per wavelength are required for accurate solutions.

A typical NASTRAN model of a duct hanger system is shown in Figure 1. Due to symmetry it was only necessary to model half of the system.

Selected mode shapes of the first 10 modes are given in Figure 2. The number of axial half-waves and circumferential waves are identified for each mode.

The FEM becomes costly when a large number of modes of a cylinder are to be considered. This is because each wave across the cylinder in both longitudinal and circumferential directions must be modeled. As the number of degrees of freedom is increased, the cost also increases. Harmonic analysis involves the inversion of the complex matrix shown in Equation (1).

$$[-\omega^2 M + i\omega C + K]u = F \tag{1}$$

This matrix must be inverted for each frequency analyzed. For example, if one desired to compute a response every 10 Hz from 1-500 Hz, this would require 50 inversions of the complex matrix in Equation (1).

The FEM is used at low frequency (0-300 Hz) due to the high reliability and accuracy of the method. The analysis was performed at 10 Hz intervals over the frequency range. Greater accuracy in the neighborhood of resonances may be obtained by using a finer frequency increment. The results of this harmonic analysis provides a basis of comparison for other more cost effective methods discussed subsequently.

Component Mode Synthesis

In order to improve accuracy and efficiency of the FEM, it is possible to provide a modal description for a component when the associated natural frequencies and mode shapes are known. Component mode synthesis (CMS) is a method which allows the cylinder to be described in terms of modes and the duct hanger assembly to be modeled with finite elements. Since the majority of the degrees of freedom of the finite element model are associated with the cylindrical duct, it is desirable to replace the finite element model of the duct by a modal representation. Fortunately, the natural frequencies and modes of a cylinder are well known (Reference 2). Donnell shell theory was selected on the basis of accuracy, especially for the mid-frequency range of this analysis.

The duct of the HVAC test section consists of a steel duct with end flanges. Typical values for properties used in analyzing the duct are given in table I.

For short cylinders (L/R < 8, L = Length of cylinder, R = Radius), there are three mode classifications: torsional, bending and coupled radial-axial modes. The nodal pattern for selected radial-axial modes is depicted in Figure 3.

In addition to the linear elastic thin shell assumptions, it is assumed that the ends of the cylinder have shear diaphragm boundary conditions. This boundary condition is equivalent to that of a simply supported beam and is reasonable in the present analysis since the sections selected terminate with flanges on each end.

Donnell Shell Theory yields the following solution for natural frequencies of axial-radial modes as Equation (2) (Reference 2):

$$f_{mn} = \frac{\lambda_{mn}}{2\pi R}\left[\frac{E}{\rho_s(1-\nu)^2}\right]^{1/2} \tag{2}$$

$$\lambda_{mn} = \frac{\left\{(1-\nu)^2\left(\frac{m\pi R}{L}\right)^4 + \left(\frac{h^2}{12R^2}\right)\left[n^2 + \left(\frac{m\pi R}{L}\right)^2\right]^4\right\}^{1/2}}{\left(\frac{m\pi R}{L}\right)^2 + n^2} \tag{3}$$

Combining (2) and (3) obtain the form of Equation (4)

$$f_{mn} = \left[\frac{\pi^2 E h^2}{48(1-\nu)\rho_s}\left(\left(\frac{m}{L}\right)^2 + \left(\frac{n}{\pi R}\right)^2\right)^2 + \frac{Em^4}{4\pi^2 R^2 \rho_s L^4}\left(\left(\frac{m}{L}\right)^2 + \left(\frac{n}{\pi R}\right)^2\right)^{-2}\right]^{1/2} \tag{4}$$

The first term under the radical of Equation (4) may be identified as the natural frequency of a flat plate. Thus, it is observed that the natural frequency of the cylinder is based on the sum of the bending term of a flat plate and a membrane term for the cylinder which acts to increase the frequency above that of a flat plate.

Mode shapes used in CMS analysis include tangential and radial components of Reference 2, shown in Equations (5) and (6), respectively:

$$v = B \sin n\theta \sin \frac{m\pi x}{L} \tag{5}$$

$$w = C \cos n\theta \sin \frac{m\pi x}{L} \tag{6}$$

The generalized masses for beam bending modes and cylinder modes are given by Equations (7) and (8), respectively.

$$M_{mn} = \frac{M}{2} \qquad m = 1, 2, 3 \ldots \; n = 1 \tag{7}$$

$$M_{mn} = \frac{M}{4} \qquad m = 1, 2, 3 \ldots \; m = 0, 2, 3, 4 \tag{8}$$

Given the eigenvalue of Equation (2) and the generalized mass of Equations (7) and (8) the determination of the generalized stiffness and damping terms are straightforward.

Since mode shape magnitudes are arbitrary, C was set equal to 1 and B/C was computed based on Equations (9) through (11).

$$\frac{B}{C} = \frac{a_{33}\, a_{21} - a_{31}\, a_{23}}{a_{22}\, a_{31} - a_{32}\, a_{21}} \tag{9}$$

where

$$a_{11} = -\xi^2 - \frac{(1-\nu)}{2} n^2 + \lambda^2 \qquad a_{12} = \frac{(1+\nu)}{2} \xi n$$

$$a_{22} = -\frac{(1-\nu)}{2} \xi^2 + \lambda^2 - n^2 \qquad a_{23} = -n$$

$$a_{13} = \nu\xi \qquad a_{31} = -\nu\xi \tag{10}$$

$$a_{21} = a_{12} \qquad a_{32} = n$$

$$a_{33} = 1 + k\,(\xi^2 + n^2)^2 - \lambda^2$$

and

$$\lambda^2 = \frac{\rho s\,(1-\nu^2)\, R^2\, \omega^2}{E}$$

$$k = \frac{h^2}{12R^2} \tag{11}$$

$$\xi = \frac{m\pi R}{L}$$

The procedure for coupling the modal representation of a component with the finite element model of any arbitrary structure is found in Section 14 of the NASTRAN Theoretical Manual (Reference 3). Briefly, the finite element model of any grid points not associated with the duct are not affected. The degrees of freedom (DOF) associated with the duct are removed by multipoint constraints which replace the DOF of the grid by a summation of modal coordinates. The response of these modal coordinates is governed by the scalar spring-mass-damper system consisting of the generalized mass, stiffness and damping associated with each mode. In other words, the duct response at each desired point of the duct

has been replaced by an eigenvector expansion. In this way, the size of the matrix required for the duct is limited to the number of modes kept in the analysis. For the duct configuration of Figure 1, 30 modes are required for 20-1000 Hz analysis.

This method has a much greater efficiency than the finite element method, allowing computation from (20-1000 Hz) in the same CPU time required for 0-300 Hz by the FEM. The analysis was performed at 10 Hz increments over the frequency range of 20 to 1,000 Hz. Greater accuracy in the neighborhood of resonances may be obtained by using a finer frequency increment.

Statistical Energy Analysis

The basic assumption used in SEA analysis is that within each band the modes are receiving energy equally. It is further assumed that the ratio of energy transmitted to modes in adjoining sections is the same for all modes within a band. Additional background regarding the SEA technique is found in References 4 and 5.

Analysis is performed by solving for the steady state energy conservation of the sections of the duct. In view of the influence of flanges on duct vibration, an appropriate procedure is to segregate duct resonances into modal groups by duct sections between flanges. For this purpose the duct test model was divided into 2 sections as shown in Figure 4.

A schematic of the mechanical energy transmission within the duct is shown in Figure 5.

Energy levels into section 1 (P_F) may be computed as follows. The desired source parameter is the net time averaged mechanical power transmitted to the set of duct structural modes. In complex notation this input power is given by:

$$P_F = 1/2 \text{ Real } \{F\ v^*\} \qquad (12)$$

where: "Real" signifies taking the real part of the bracketed complex product and

F = magnitude of applied force to the duct

v^* = complex conjugate of resulting duct velocity

The relation between force and velocity was provided by the impedance of an infinite elastic cylindrical shell (Reference 6).

Of this energy some is lost due to damping in the duct (P_i^D), a certain amount is transferred to adjoining sections (P_{ij}) and the remainder is retained as vibration energy.

Applying the principle of conservation of energy establishes the relationship for the ith model system as:

$$\text{Net input power } P_i{}^i{}_n = P_i^D + P_i^H + \sum_j P_{ij} \qquad (13)$$

The power dissipated in the ith system can be expressed as:

$$P_i^D = \omega \eta_i^D E_i \tag{14}$$

where η_i^D is the dissipation loss factor. The power transferred to the hanger is represented in similar fashion, i.e.,

$$P_i^H = \omega \eta_i^H E_i \tag{15}$$

where η_i^H is the loss factor of the hanger system.

The power transferred to and from adjacent systems is given by:

$$P_{ij} = \omega \eta_{ij} - \omega \eta_{ji} E_i \tag{16}$$

The set of above equations as applied to each of the three identical mode sets is conveniently represented in matrix form as:

$$\omega[\eta]\{E\} = \{P\} \tag{17}$$

where: $\{E\}$ is a column matrix of subsystem total energies

$\{P\}$ is a column matrix of subsystem input power and

$[\eta]$ is a square matrix of dissipation, and coupling loss factors

The coupling loss factors were taken from Reference 4 and the damping loss factor used was that given in Reference 7.

For each 1/3 octave band frequency, the power into the forced section of the duct is given by Equation (12). The corresponding matrix equation can then be solved for the model energies of each system for each 1/3 octave band; e.g.,

$$\{E\} = \frac{1}{\omega}[\eta]^{-1}\{P\} \tag{18}$$

Structural Response

The average velocity associated with each duct section may be obtained from the energy of that section as follows:

$$\bar{v} = \sqrt{\frac{2E}{m}} \tag{19}$$

where m is the mass of the cylinder.

In order to perform accurate statistical energy analysis (SEA) , it is necessary to consider the number of modes for each component of the system in the frequency range of interest (10-5000 Hz). For example, consider the typical duct configuration of Figure 1. This system has four components; the cylinder, mount, hanger and foundation. The geometric and material properties of the duct, mount, and hanger are provided in tables I through III. The foundation impedance was taken to be a 0.5-inch infinite steel plate. Shell theory of Donnell predicts 300 modes of the duct section in the frequency range of interest. There are four modes per 1/3 octave band beginning at 800 Hz. The

number of modes in all other components is limited to one or no modes per 1/3 octave band.

In view of the number of modes for each component given above, consider the SEA method. Based on the number of modes per 1/3 octave band for the cylinder, the SEA method is applicable at and above 800 Hz. Due to the low mode count for the remaining components, it would be inappropriate to attempt to represent the mount, hanger, or foundation as a modal subsystem. However, the effect of the hanger assembly on the cylinder may be included through the use of a coupling loss factor. The computation of a loss factor to represent power flow from the cylinder to the hanger assembly was obtained from an analysis of the hanger assembly shown in Figure 6. The method used to obtain the loss factor was that of the Dynamic Direct Stiffness Method (DDSM). This method also provides transfer functions between the response of the cylinder at the attachment point and the response of points along the hanger assembly and foundation. Following SEA analysis of the cylinder, these transfer functions were used to relate the cylinder response to the desired responses of the duct hanger and foundation.

Dynamic Direct Stiffness Method

In order to effectively analyze hanger designs over a large range of frequencies, the DDSM (Direct Dynamic Stiffness Method) was used. A detailed derivation of the method is found in Reference 8. Basically, the method involves a matrix representation of a beam (or network of beams) which is frequency dependent and is an exact solution to the fourth order flexural beam equation for harmonic excitation. A computer program has been developed by NKF to create and solve the system of equations for the DDSM. The computer program has been enhanced to include models for isolators, and attached impedances of infinite beams, plates and cylinders.

RESULTS OF ANALYSIS

In order to demonstrate the methodology just described, the duct section shown in Figure 1 was analyzed. The hanger system consists of a pipe modeled with beams, and an isolator modeled as a beam. The cylinder was modeled with CQUAD elements in the case of the FEM and with Donnell shell eigensolutions for the CMS and SEA methods. The system was harmonically excited by a unit concentrated radial force located 11 inches in from the end of the duct.

The results computed include the velocities on the cylinder and hanger system and the power flow from the excitation through an impedance representing a foundation attachment. The impedance of the foundation in this case was taken to be that of an infinite 1/2-inch steel plate.

The results for the velocity on the duct are presented in Figures 7 and 8. It is observed that the FEM and CMS solutions show reasonable agreement. The main reason for discrepancy is that the CMS method is based on Donnell shell theory which tends to give a low frequency estimate for the first few cylinder modes. Donnell shell theory frequency estimates improve rapidly with wave number. Since the modal mass is fixed per Equations (7) and (8), a low estimate of frequency results in a low stiffness and consequently an estimate of velocity which is slightly conservative. The SEA results are the average velocities over

the cylinder and are only expected to be accurate when there are at least four modes in a band (above 800 Hz). When comparing the CMS and SEA velocities in the 800-1000 Hz range, it is observed that the velocity of the drive point is greater for CMS than for SEA, as expected. In the case of the velocity at the duct below the mount shown in Figure 8, there appears to be only one predominant mode out of several modes in the 800-1000 Hz band. For this reason the CMS prediction is higher than that given by SEA. It is expected that as the analysis of CMS is extended beyond 1000 Hz, the CMS method would approach the SEA solution.

The velocities for the duct hanger system are shown in Figures 9 and 10. The velocity directly above the mount, shown in Figure 9, shows reasonable correlation between all three methods. Again, the appropriate range of comparison between methods is relatively narrow, 0-300 Hz for FEA versus CMS and 800-1000 Hz for CMS versus SEA.

The results for the termination point are shown in Figure 11. The velocities in this case are associated with the axial velocity of the duct hanger at the attachment point to the foundation. It is observed in Figure 11 that there are few modes participating, even in the 800 Hz band. For this reason, the CMS and SEA analyses have not converged. It is anticipated that as the analysis is extended above 1000 Hz, that the CMS analysis would approach the SEA solution.

The power flow results for the axial power flow through the duct hanger into the foundation per unit force of input to the duct are given in Figure 12. The SEA force power magnitudes are low by as much as 10 dB in agreement with the axial termination velocities. The same comments made for Figure 11 apply in this case as well.

The moment power flow results through the duct hanger system to the foundation are shown in Figure 13. In this case the SEA results match closely with the CMS and FEA results.

The analysis presented here involved the following computation times on a VAX 11/780:

- FEA - 8 hours, 0-500 Hz
- CMS - 4 hours, 0-1000 Hz
- SEA - 1 hour, 0-5000 Hz

The relative efficiency and accuracy of each method is now apparent. For a very accurate analysis of the low frequency range, the FEA method is affordable while the CMS method is reasonably accurate for the mid-range and the SEA method is appropriate at the high end of the spectrum.

CONCLUSIONS

In this paper several methods have been presented which, together, may be used in the analysis of duct hanger systems over a wide range of frequencies. The FEM and CMS methods are used for low- to mid-frequency range computations and have been shown to yield reasonably close results. The SEA method yields

predictions which agree with the CMS results for the 800-1000 Hz range provided that a sufficient number of modes participate. The CMS approach has been shown to yield valuable insight into the mid-frequency range of the analysis. It has been demonstrated that it is possible to conduct an analysis of a duct/hanger system in a cost-effective manner for a wide frequency range, using several methods which overlap for several frequency bands. Using several methods in this way gives a high degree of confidence in the results.

REFERENCES

1. McCormick, C.W., "The NASTRAN User's Manual (Level 17.5)."

2. Blevins, R., "Formulas for Natural Frequency and Mode Shape," Van Nostrand Reinhold Co., New York, 1979.

3. MacNeal, R.H., "The NASTRAN Theoretical Manual (Level 17.5)."

4. Lyon, R., "Statistical Energy Analysis of Dynamical Systems: Theory and Applications," The MIT Press, 1975.

5. Miller, R.D. and Kasper, P.K., "Underwater Radiated Noise of a Stiffened Shell: Analytical Methodology Using a Combined Formulation," 57th Shock and Vibration Symposium, 15 October 1986.

6. Heckle, M., "Vibrations of Point-Driven Cylindrical Shells," J. Acoust. Soc. Am. 34, 1553-1557, 1962.

7. Cremer, L., M. Heckle, and E. Ungar, "Structureborne Sound," Springer-Verlag, 1973.

8. Clough and Penzien, "Dynamics of Structures," McGraw-Hill, New York, 1975.

TABLE I.- DUCT PROPERTIES

Property	Value
Shell Thickness	h = 0.05 in.
Section Length (x2 Sections)	L = 40 in.
Section Radius	R = 4 in.
End Flanges	
Cross-Sectional Area	0.05 in^2
Second Moment of Area	0.00417 in^4

TABLE II.- MOUNT PROPERTIES

Property	Value
Young's Modulus	$E = 555\ lb/in^2$
Shear Modulus	$G = 189.7\ lb/in^2$
Weight Density	$\gamma = 0.0420\ lb/in^3$
Cross-Sectional Area	$A = 0.500\ in^2$
Second Moment of Area	$I = 0.0420\ in^4$

TABLE III.- DUCT HANGER PROPERTIES

Property	Value
Young's Modulus	$E = 30.0\ E{+}6\ lb/in^2$
Shear Modulus	$G = 11.5\ E{+}6\ lb/in^2$
Weight Density	$\gamma = 0.283\ lb/in^3$
Cross-Sectional Area	$A = 0.785\ in^2$
Second Moment of Area	$I = 0.0491\ in^4$

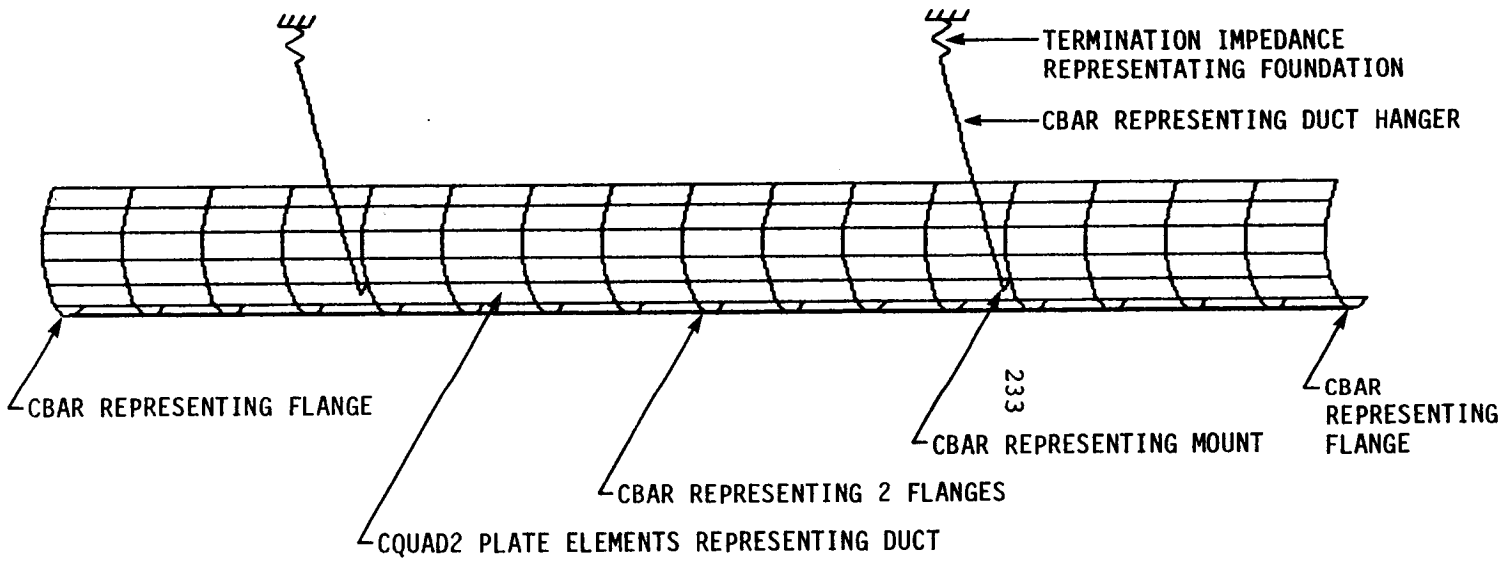

FIGURE 1.- TYPICAL NASTRAN MODEL OF A DUCT HANGER TEST CONFIGURATION

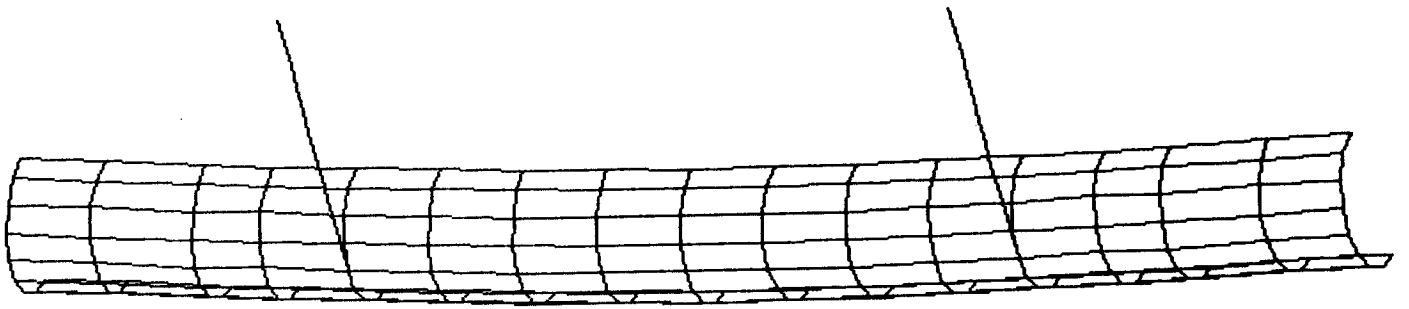

FIRST DUCT BEAM BENDING MODE (m=1, n=1) (144.7 Hz)

FIGURE 2.- TYPICAL DUCT HANGER SYSTEM MODAL ANALYSIS (SHEET 1 OF 5)

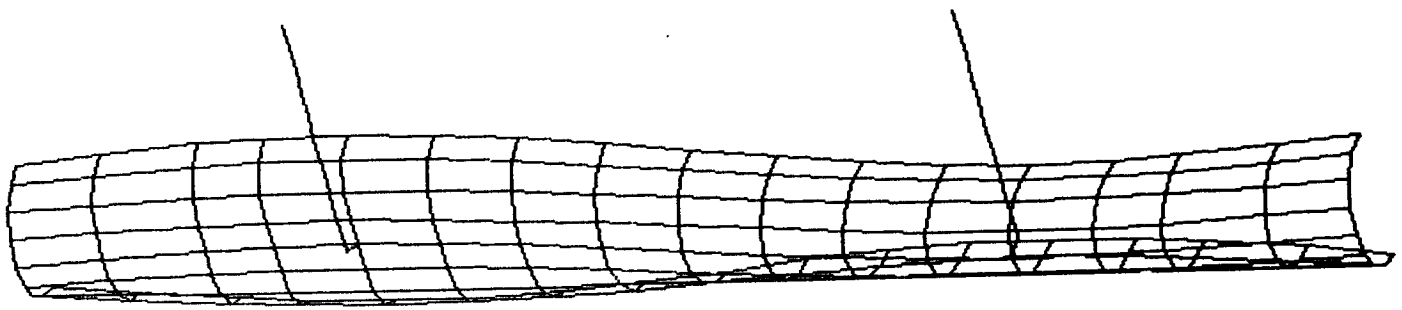

ASYMMETRIC TWO-AXIAL HALF WAVES, TWO CIRCUMFERENTIAL WAVES MODE (m=2, n=2) (241.3 Hz)

FIGURE 2.- TYPICAL DUCT HANGER SYSTEM MODAL ANALYSIS (SHEET 2 OF 5)

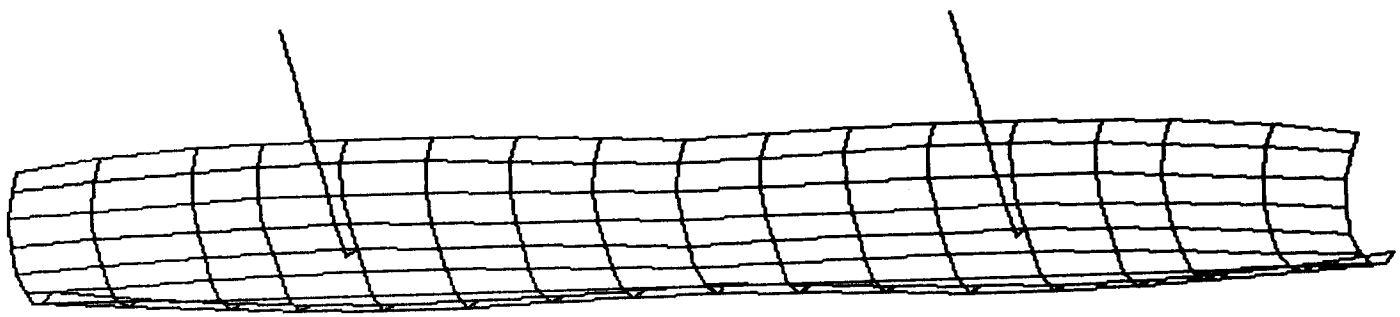

SYMMETRIC TWO-AXIAL HALF WAVES, TWO CIRCUMFERENTIAL WAVES MODE (m=1, n=1) (269.4 Hz)

FIGURE 2.- TYPICAL DUCT HANGER SYSTEM MODAL ANALYSIS (SHEET 3 OF 5)

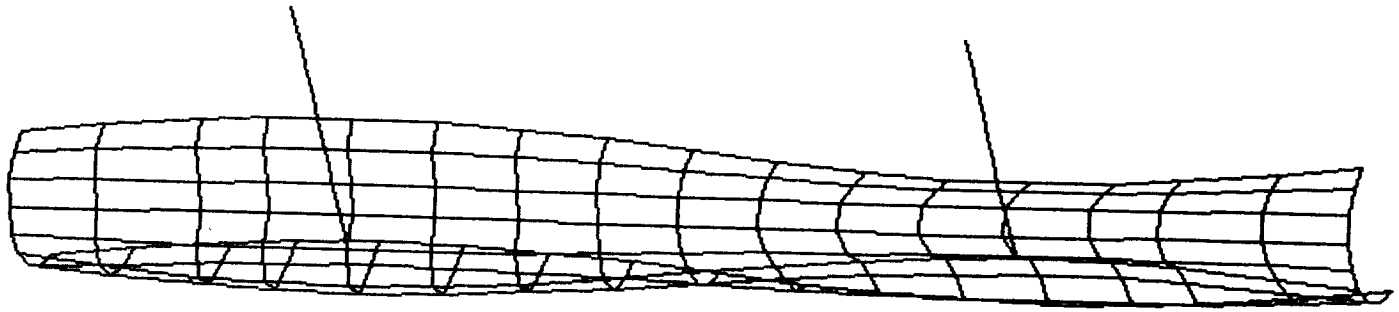

ASYMMETRIC TWO-AXIAL HALF WAVES, THREE CIRCUMFERENTIAL WAVES MODE (m=2, n=3) (281.3 Hz)

FIGURE 2.- TYPICAL DUCT HANGER SYSTEM MODAL ANALYSIS (SHEET 4 OF 5)

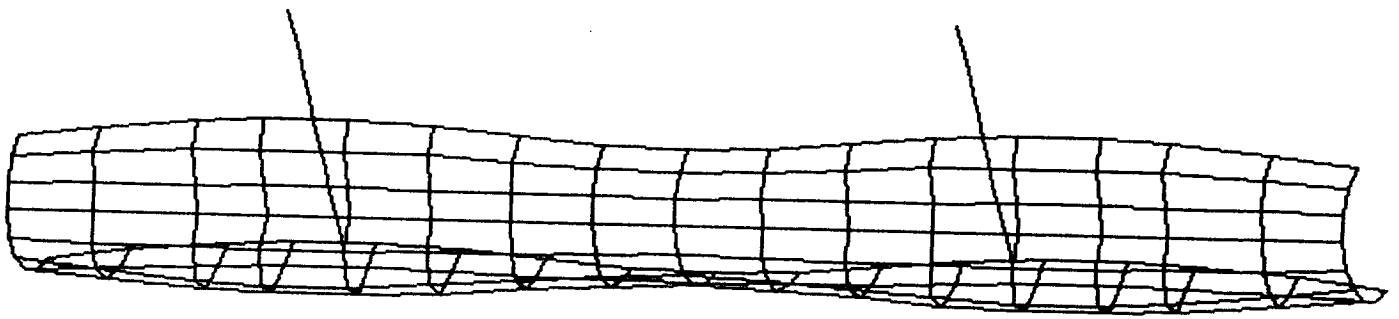

SYMMETRIC TWO-AXIAL HALF WAVES, THREE CIRCUMFERENTIAL WAVES MODE (m=2, n=3) (318.0 Hz)

FIGURE 2.- TYPICAL DUCT HANGER SYSTEM MODAL ANALYSIS (SHEET 5 OF 5)

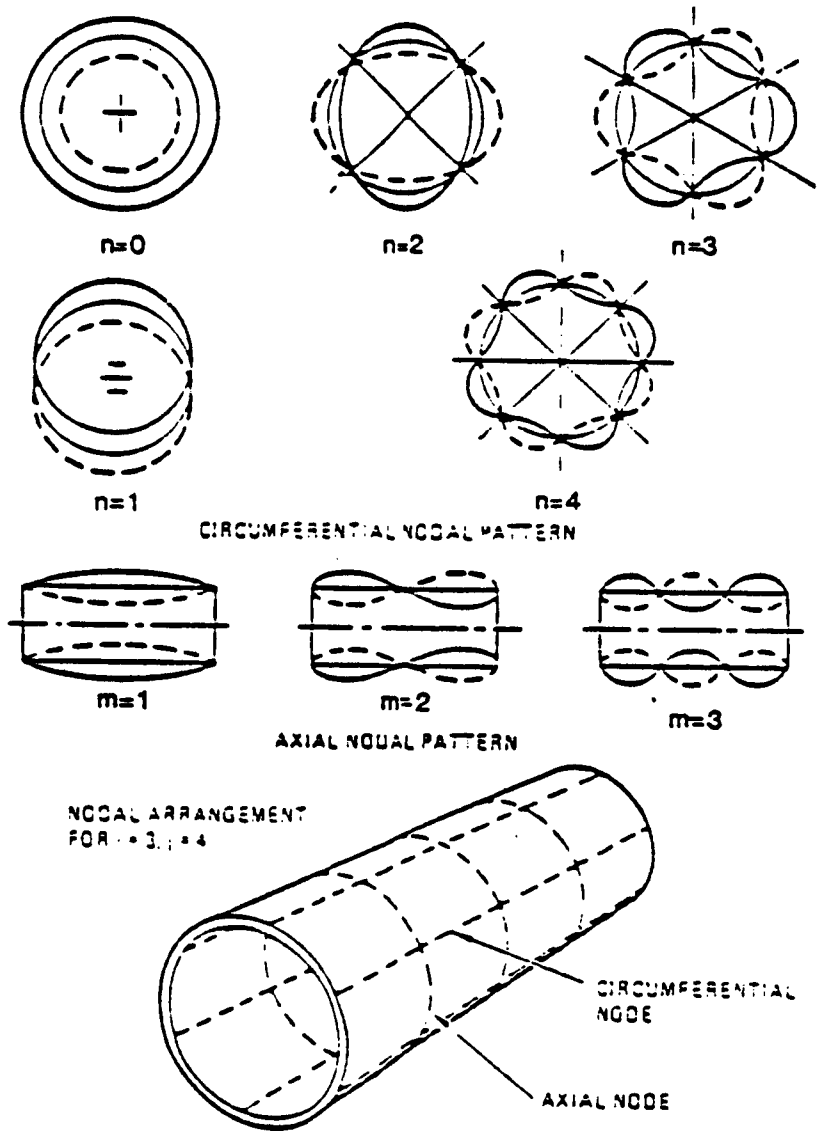

m = Number of Axial Half-Waves

n = Number of Circumferential Waves

FIGURE 3.- NODAL PATTERNS FOR A SIMPLY SUPPORTED CYLINDER WITHOUT AXIAL CONSTRAINTS (REFERENCE 2)

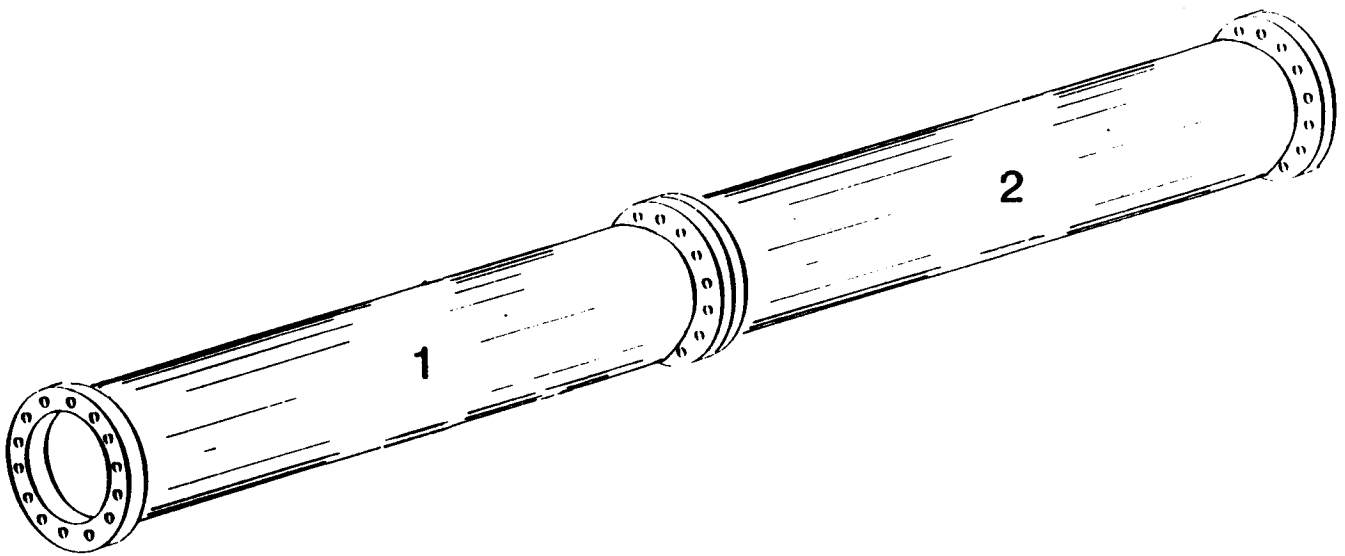

FIGURE 4.- TYPICAL DUCT SECTIONS

P_i^D =POWER DISSIPATED BY DUCT DAMPING

P_i^H =POWER TRANSFERED TO DUCT HANGER

P_{ij} =POWER TRANSFERRED BETWEEN SECTION i AND j

P_F =VIBRATION POWER TRANSMITTED BY POINT FORCE

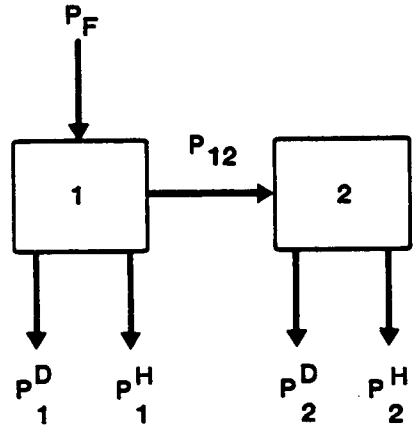

FIGURE 5.- SCHEMATIC REPRESENTATION OF SEA MODEL OF A DUCT HANGER SYSTEM BY MODAL SUBSYSTEMS

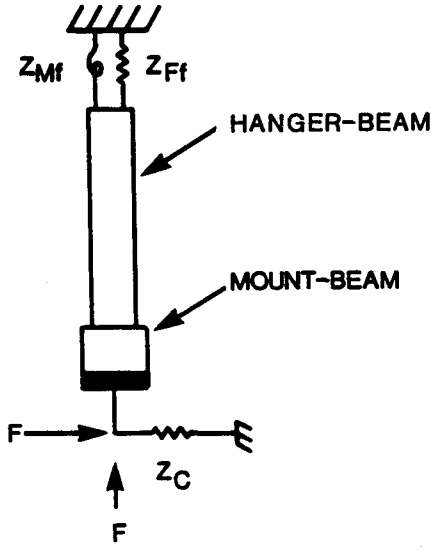

Z_{mf} = POINT MOMENT FOUNDATION IMPEDANCE

Z_{Ff} = POINT FORCE FOUNDATION IMPEDANCE

Z_C = INFINITE CYLINDER IMPEDANCE

FIGURE 6.- DUCT HANGER ASSEMBLY/FOUNDATION MODEL

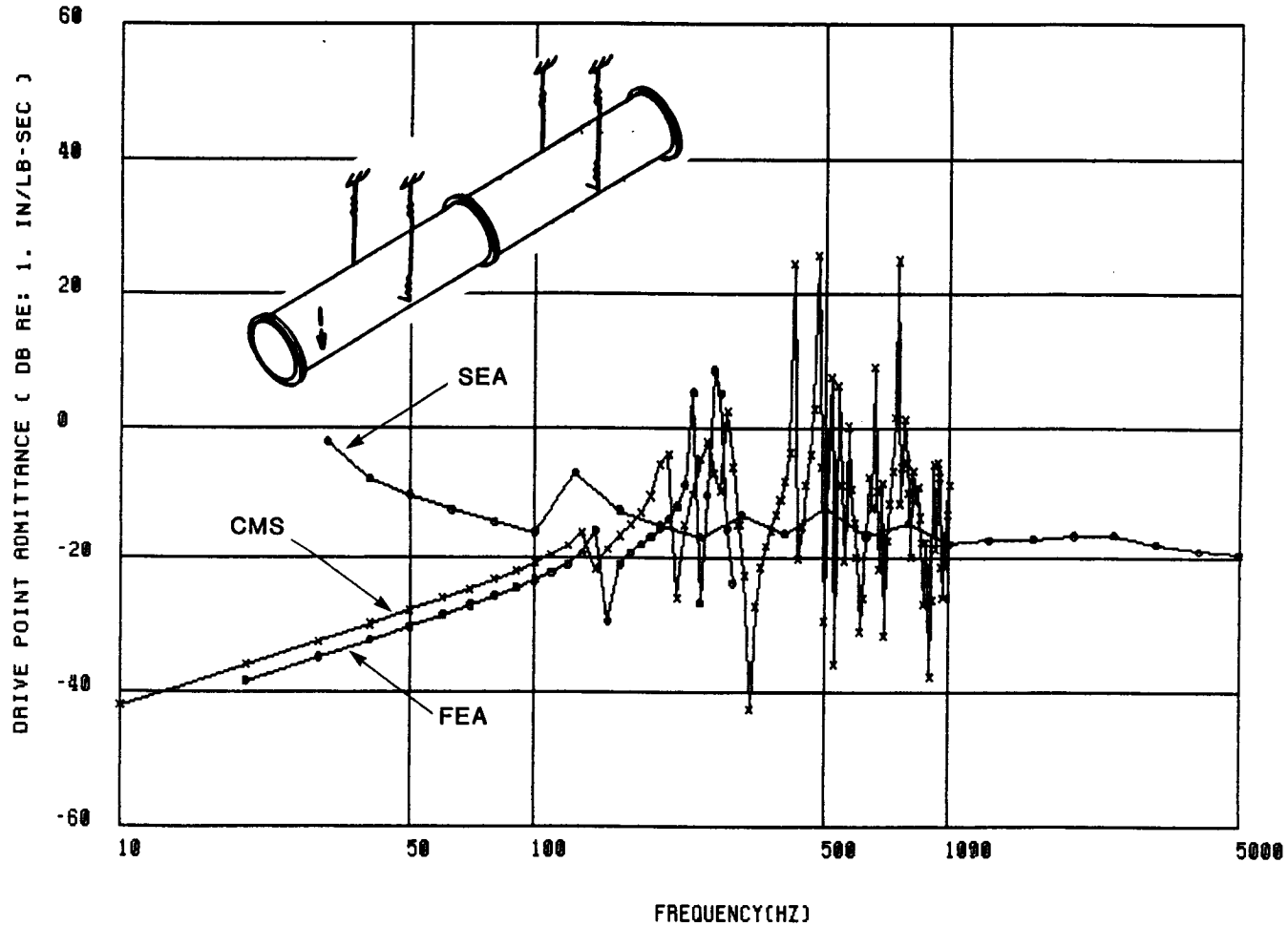

FIGURE 7.- FEA AND CMS DRIVE POINT ADMITTANCE VS. SEA AVERAGE DUCT VELOCITY

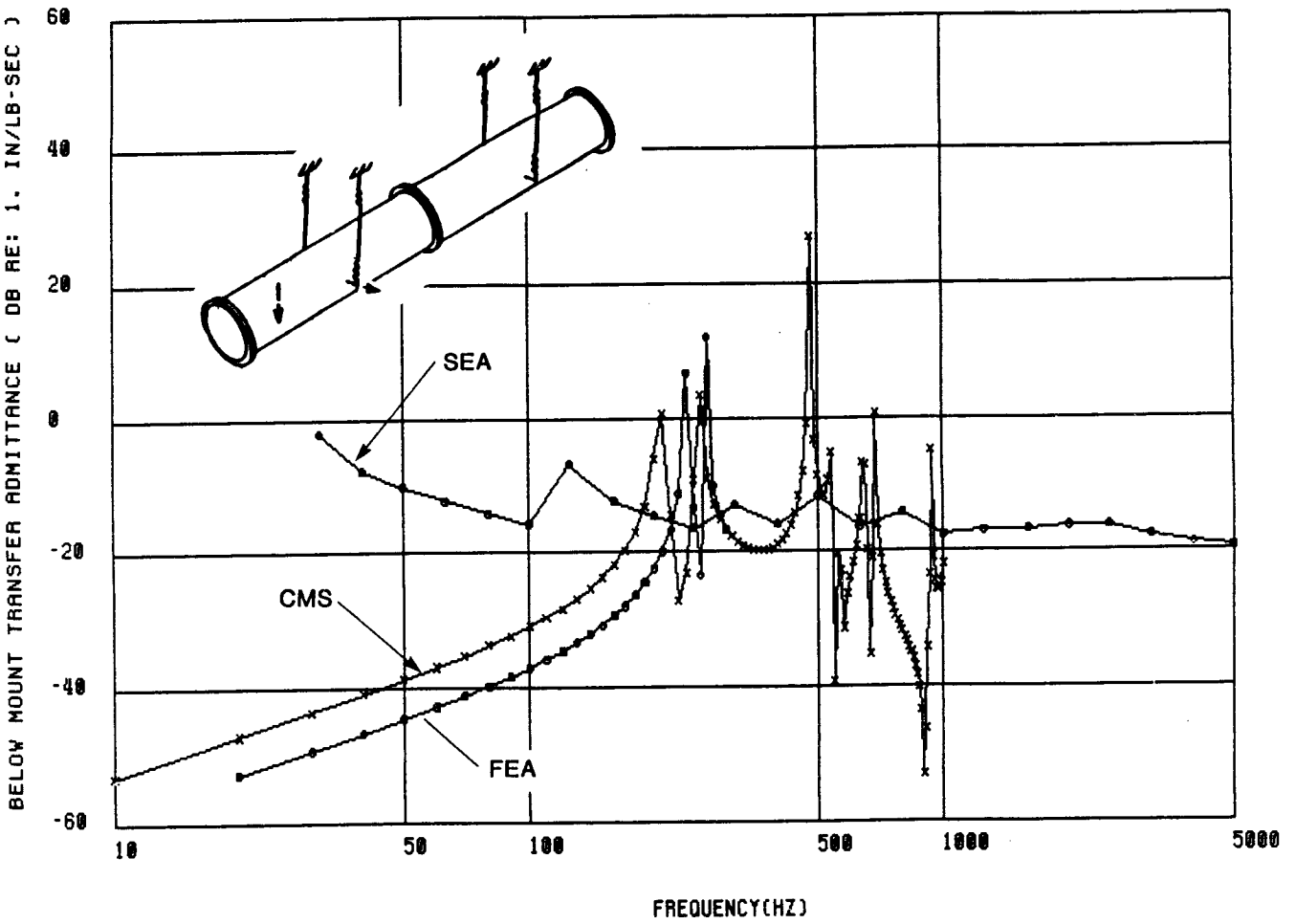

FIGURE 8.- RADIAL TRANSFER ADMITTANCE AT DUCT BELOW MOUNT

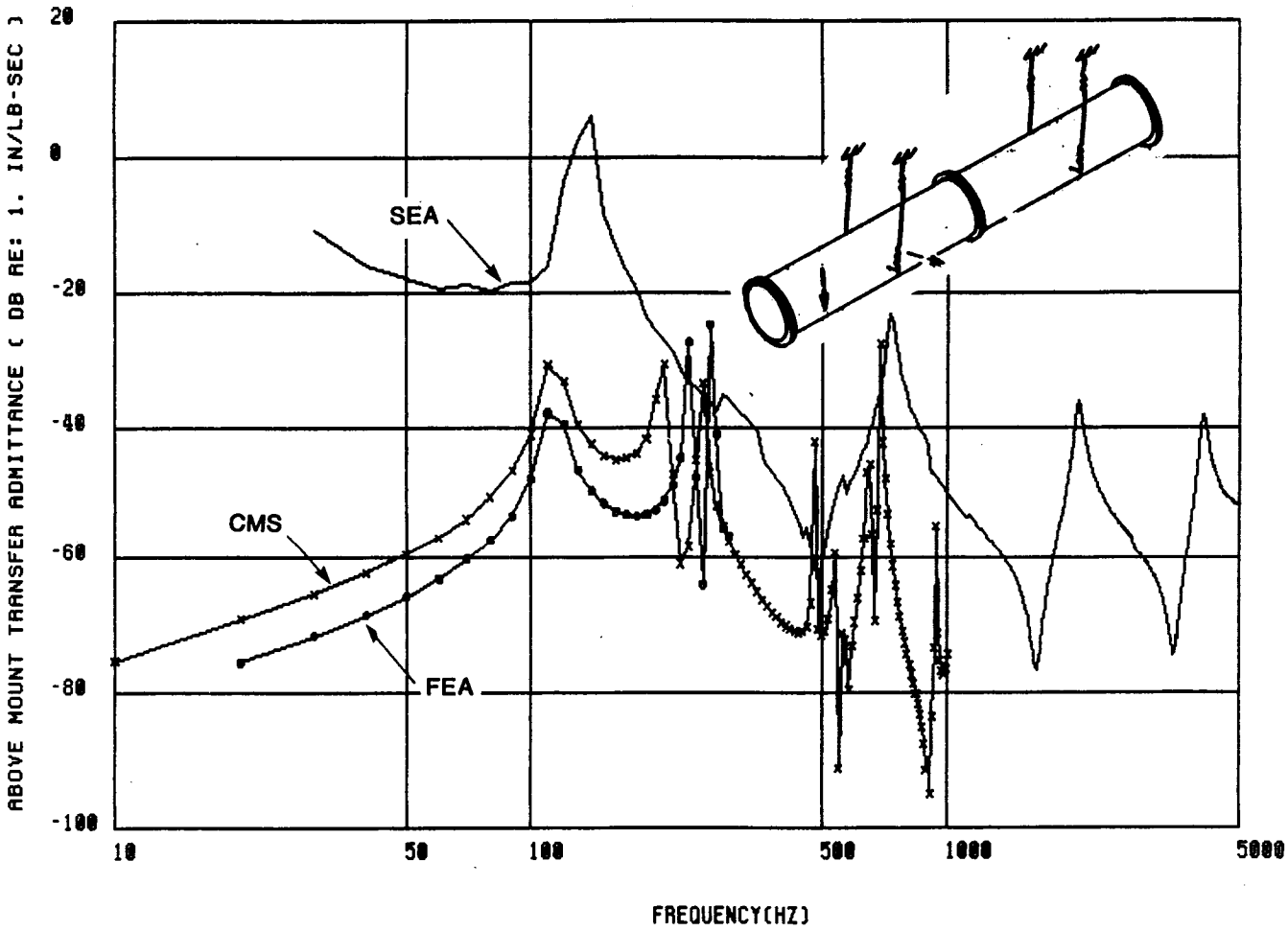

FIGURE 9.- TRANSVERSE TRANSFER ADMITTANCE AT HANGER ABOVE MOUNT

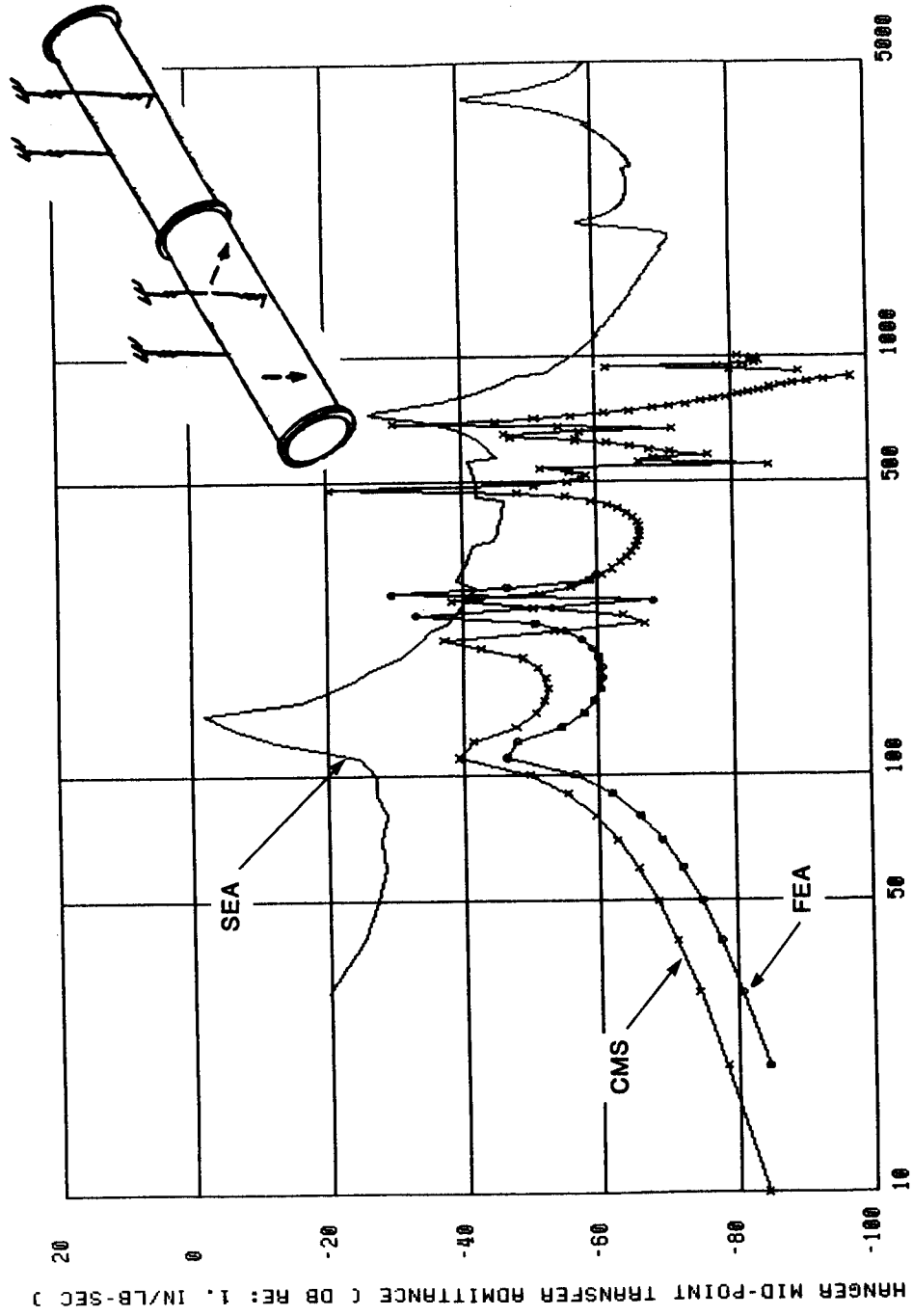

FIGURE 10.- TRANSVERSE TRANSFER ADMITTANCE AT HANGER MIDPOINT

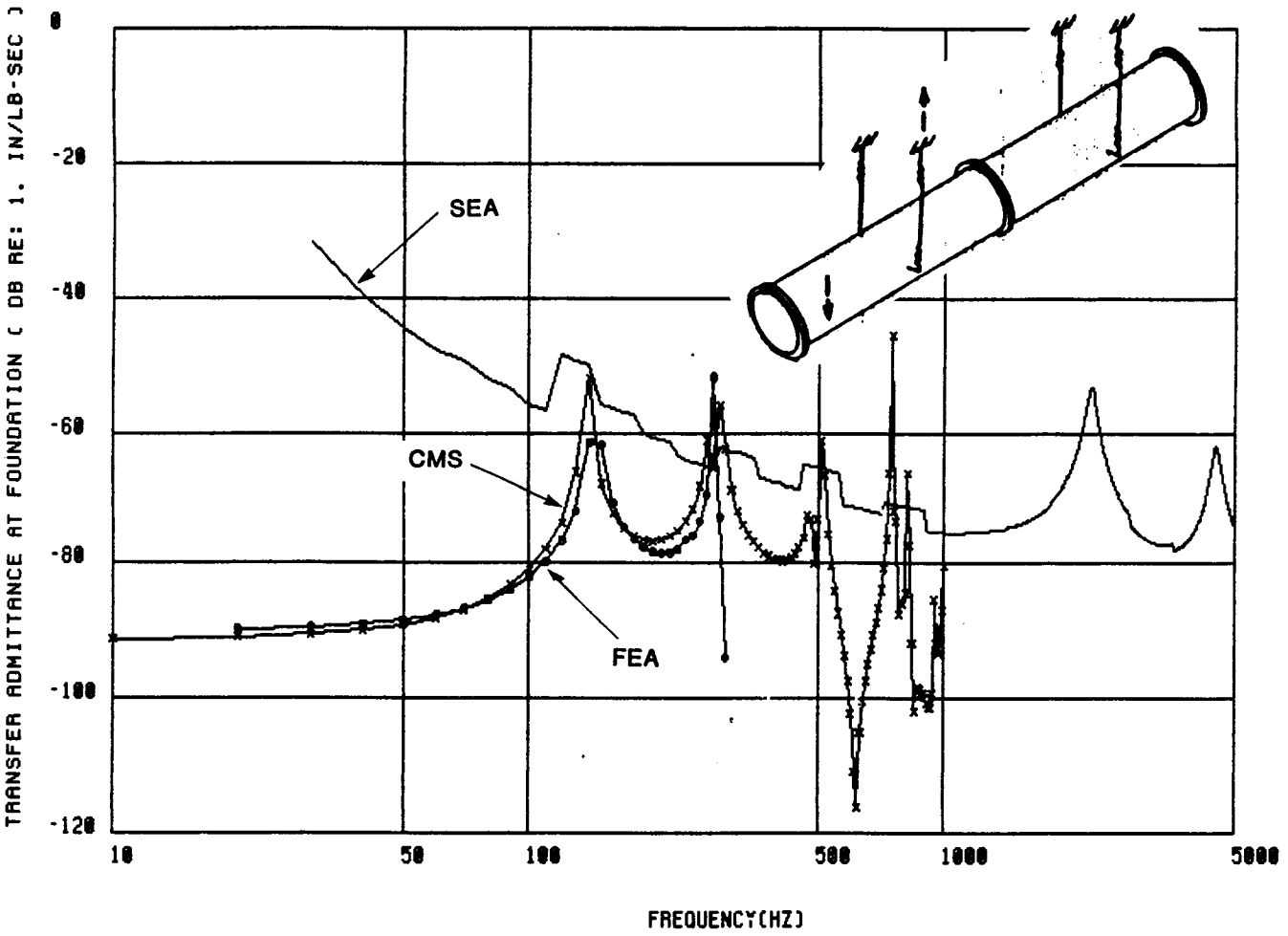

FIGURE 11.- VERTICAL TRANSFER ADMITTANCE AT FOUNDATION

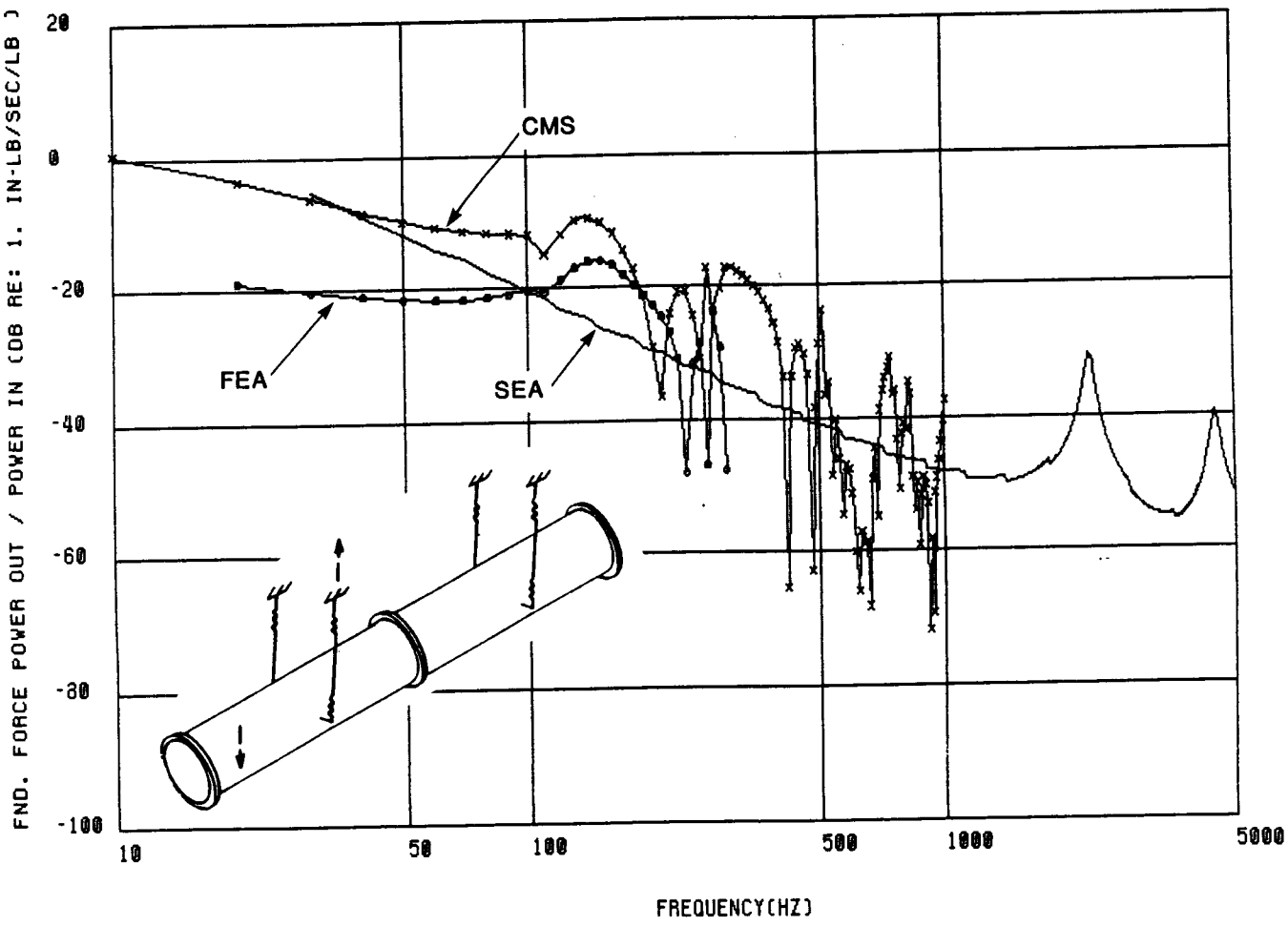

FIGURE 12.- FOUNDATION FORCE POWER OUT/POWER IN

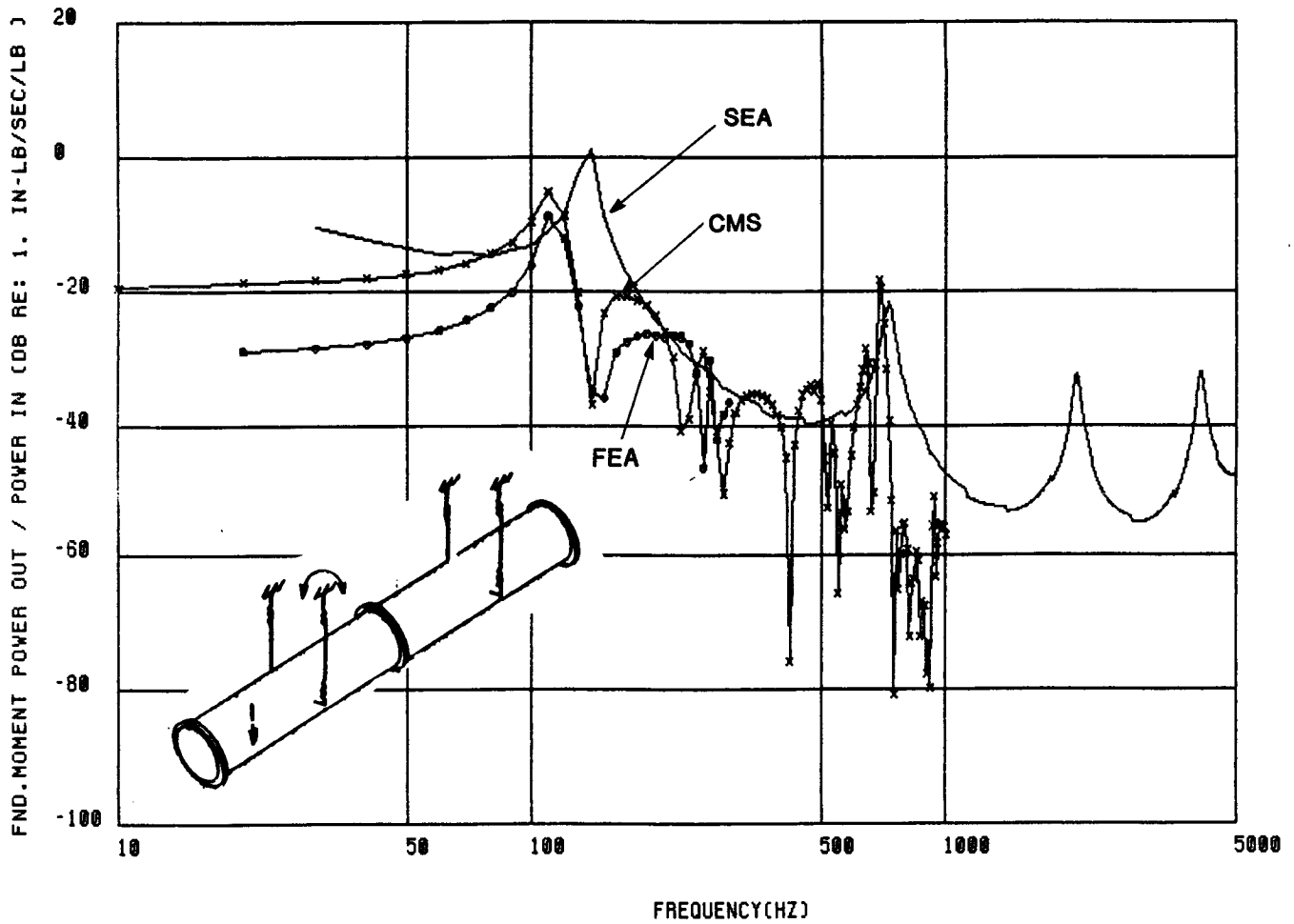

FIGURE 13.- FOUNDATION MOMENT POWER OUT/POWER IN